Symmetry-extended mobility counting for plate-bar systems, with applications to rod-bar and rod-clamp frameworks

Bernd Schulze*

Department of Mathematics and Statistics
Lancaster University, Lancaster LA1 4YF, UK
b.schulze@lancaster.ac.uk

Patrick W. Fowler

Department of Chemistry
University of Sheffield
Sheffield S3 7HF, UK
p.w.fowler@sheffield.ac.uk

Simon D. Guest

Department of Engineering
University of Cambridge
Trumpington Street, Cambridge CB2 1PZ, UK
sdg@eng.cam.ac.uk

Abstract

We obtain symmetry-extended counting rules for the mobility of general *plate-bar* frameworks in configurations with non-trivial point-group symmetry. Necessary conditions for isostaticity of a symmetric rod-bar framework in 3-space are derived. An example shows that establishing sufficient conditions will require significant further development. A symmetry-extended counting rule is established for *rod-clamp* frameworks: plate-bar frameworks are clamped in such a way as to remove relative translations within clamped pairs. Worked examples showing the utility of the symmetry approach in detecting mechanisms and states of self-stress include an application to linear

pentapods where a singular configuration is detected by symmetry.

Keywords: rigidity, plate-bar framework, rod-bar framework, rod-clamp framework, symmetry, linear pentapod

1. Introduction

The notion of a plate-bar framework (Kiraly and Tanigawa, 2019; Tay, 1991; Tanigawa, 2012) provides a useful generalisation of a number of classical structural models and gives a context for discussion of questions of generic rigidity of different model types.[1] For a given dimension d and integer $k \leq d$, a *k-plate* is a k-dimensional rigid body in d-space. A d-dimensional plate-bar framework consists of a set of k-plates, where k can take values between 0 and d, and where these plates are connected together by rigid *bars*, each of which provides a length constraint between two joints that lie on different plates.

Often the most interesting cases are the (d, k)-plate-bar frameworks, where all plates for the given framework embedded in d-dimensional space share a common value of k. We could consider this as the 'regular limit' of a general case where sets of plates of different dimensions are present together. Specific parameter values for this regular case correspond to well known systems in $d = 2$ and 3 dimensions, such as the bar-joint frameworks ($k = 0$) and the body-bar frameworks ($k = d$). See Tay (1984); Whiteley (1996) for definitions and examples. If $d = 3$ and $k = 1$ we have the case of a *rod-bar framework* in 3-space (Tay, 1991; Tanigawa, 2012). Thus, body-bar,

[1]Our interest in working with this generalisation was sparked by a talk on 'Combinatorics of Body-Bar-Hinge Frameworks' given by Shin-ichi Tanigawa at the meeting on Bond-Node Structures at Lancaster University in 2018.

panel-bar and rod-bar frameworks correspond to 3-plate-bar, 2-plate-bar and 1-plate-bar systems, respectively.

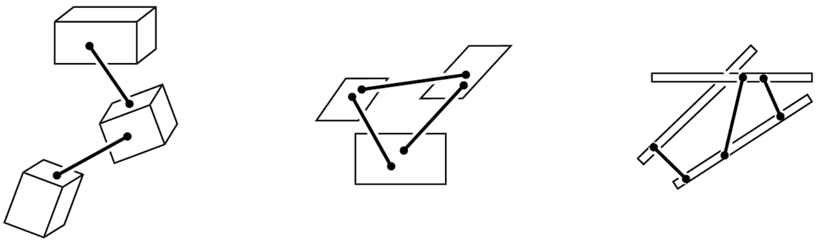

(a) (b) (c)

Figure 1: Frameworks in 3-space: (a) A *body-bar* framework, (b) a *panel-bar* framework, and (c) a *rod-bar* framework. Dumbbell symbols indicate a bar and its two points of attachment.

The focus of the present paper is on the use of a symmetry-based approach to enrich and give insight into the various counting rules that govern the balance of mechanisms and states-of-self-stress in these plate-bar frameworks. Previous work in this area on other types of framework (e.g., bar-joint frameworks (Guest and Fowler, 2007; Connelly et al., 2009), body-bar frameworks (Guest et al., 2010) and body-hinge frameworks (Guest and Fowler, 2010; Schulze et al., 2014; Chen et al., 2016, 2012) has shown how fruitful this approach can be in aiding detection and understanding of 'hidden' mechanisms and their persistence or blocking as symmetry is lowered along some distortive pathway. In each case, the generic methodology is adapted to the particular symmetry characteristics of the types of freedom and constraint encountered in the class of systems under study. This procedure is followed here.

The structure of the paper is as follows. We first review the Maxwell-type counting rules for the mobility of regular plate-bar frameworks in §2.

We then derive the corresponding symmetry-extended counting rules in §3. In §4, we apply these new rules to a number of examples. Necessary conditions for a symmetric rod-bar framework in 3-space to be isostatic (i.e., minimally rigid or, equivalently, maximally self-stress-free) are established in §5, following the approach taken in Connelly et al. (2009) and Guest et al. (2010) for bar-joint and body-bar frameworks. In §6 and §7 we discuss extensions of the symmetry-extended counting rules to the special type of rod-bar frameworks called *rod-clamp frameworks* and to mixed *body-panel-rod frameworks*, respectively. If a pair of rods in 3-space is joined by three orthogonal bars so that the three bars are coincident on a common point of the two rods, then this removes the 3-dimensional space of relative translations of the rods, resulting in a *clamp*. A structure consisting of rods that are joined in pairs by clamps is called a *rod-clamp* framework (Tay, 1991). We note that a clamp in a rod-clamp framework can equally be considered as a ball joint connecting the two rods. Finally, we investigate in §8 whether, under suitable genericity assumptions, the necessary conditions derived in §5 for isostaticity of a symmetric rod-bar framework are also sufficient.

2. Scalar counting for plate-bar frameworks

Our interest here is in the mobility of plate-bar frameworks, and specifically in how symmetry arguments can be used to sharpen rigidity conditions derived from scalar counting rules such as those of Maxwell and Kutzbach (Maxwell, 1864; Kutzbach, 1929). As in our previous implementations of this approach (Fowler and Guest, 2000; Guest and Fowler, 2005; Guest et al., 2010) we begin here by counting freedoms and constraints, then generalise to include the effects of non-trivial point-group symmetry.

We consider the contact graph of the framework, $\mathcal{C}$, where each vertex in the set $V(\mathcal{C})$ corresponds to a plate, and each edge in the set $E(\mathcal{C})$ corresponds to a bar. Note that $\mathcal{C}$ is a multigraph that may contain parallel edges, but no self-loops. We work in d dimensions, and k takes values 0 to d.

The *rigid-body motions* for Euclidean space of dimension d are of dimension $\binom{d+1}{2}$ (see, for example, Asimow and Roth (1979); Whiteley (1996)): they are spanned by a set of d translations and a set of $\binom{d}{2}$ rotations.

The *freedoms* of a set of disconnected k-plates in d dimensions arise from the translations and rotations in d dimensions of each plate, reduced by any 'ineffective' rotations that are indistinguishable from the identity operation for plates of dimension k. Note that a rotation is ineffective for a given k-plate if and only if the rotational axis contains the plate. Therefore, a $\binom{d-k}{2}$-dimensional subspace of the $\binom{d}{2}$-dimensional space of rotations in d-space has no effect on any given k-plate. The justification for this statement is that a rotation in d-space has a $(d-2)$-dimensional axis, and hence the rotation has an effect only on the remaining 2-dimensional space. Therefore, a k-plate in d-space has a total number of *degrees of freedom* equal to

$$\binom{d+1}{2} - \binom{d-k}{2}.$$

Notice that in the standard convention for binomial coefficients, the symbol $\binom{i}{j}$ with $i < j$ evaluates to 0. This needs to be borne in mind for symbols such as $\binom{d-k}{2}$. The *constraints* on the framework are those imposed by the set of $|E|$ bars.

The internal freedoms of the assembled framework follow by subtraction of constraints and trivial rigid-body motions from the freedoms of the set of disconnected plates. The mobility (the Maxwell count, calculated in the spirit of Calladine (Calladine, 1978) as the balance of mechanisms and states of self stress), for a (d, k)-plate-bar framework is therefore:

$$m - s = \left[\binom{d+1}{2} - \binom{d-k}{2}\right]|V| - \binom{d+1}{2} - |E|. \tag{2.1}$$

Note that (2.1) takes identical values for the cases $k = d - 1$ and $k = d$ with given d, as $\binom{0}{2} = \binom{1}{2} = 0$.

In non-regular cases, there may be different numbers $|V_k|$ for each k allowed by the dimensionality d. Each edge still contributes a single constraint that is symmetric under all those operations that leave this edge in place, and hence the mobility equation (2.1) generalises to (2.2)

$$m - s = \left\{ \sum_{k=0}^{d} \left[\binom{d+1}{2} - \binom{d-k}{2}\right]|V_k| - \binom{d+1}{2} \right\} - |E|. \tag{2.2}$$

The cases of physical interest are for dimensions $d = 2$ and $d = 3$. In 2D there are three regular cases, with $k = 0, 1, 2$, corresponding respectively to bar-joint, rod-bar and body-bar frameworks. The degrees of freedom in the Maxwell counts are $2v - 3$ ($k = 0$) and $3v - 3$ ($k = 1, 2$), where $v = |V|$ is the number of vertices of the contact graph. Bar-joint and body-bar frameworks are well studied; in the combination of bars with line segments, the line segments retain three degrees of freedom (two translations and one rotation), and the whole is effectively equivalent to a body-bar framework in which all bars attached to a body have collinear end points. Symmetry-extended counting rules for these structures were established in previous work (Fowler and Guest, 2000; Guest and Fowler, 2005).

In 3D, the cases range from $k = 0$ to $k = 3$. These correspond to bar-joint, rod-bar, panel-bar and body-bar frameworks (See Figure 1). The respective degrees of freedom in the Maxwell counts are $3v - 6$ ($k = 0$), $5v - 6$ ($k = 1$), and $6v - 6$ ($k = 2, 3$). Mixed systems are possible, and follow combined counting rules as in Eq. (2.2).

Remark 2.1. *In this paper, we consider generalisations of body-bar frameworks characterised by allowing bodies of lower dimension than the ambient dimension of the structure. A similar direction has been studied intensively for the class of* body-hinge frameworks*. A body-hinge framework is a special type of body-bar framework, in which each pair of bodies is either unconnected, or is connected by five bars meeting a hinge line so that only a single rotational degree of freedom (about the hinge line) between the two bodies remains (Whiteley, 1996). An important class of body-hinge frameworks is that of* panel-hinge frameworks*, where all hinge lines of a given body are coplanar (i.e., the bodies can be thought of as* 2*-dimensional panels). These structures (and their dual structures,* molecular frameworks*) have a wide range of applications in engineering and biophysics (Katoh and Tanigawa, 2011; Tay and Whiteley, 1984; Whiteley, 1996, 2005). Symmetry-extended counting rules for mobility of body-hinge structures can be found in Schulze et al. (2014).*

3. Mobility counting with symmetry

We now consider symmetric plate-bar structures in 3D, and derive symmetry-extended counting rules that generalise the scalar counting rules. In the standard Schoenflies notation (see Altmann and Herzig (1994); Atkins et al. (1970), for example) the families of 3D point groups are: the trivial group $\mathcal{C}_1$, the reflection symmetry group $\mathcal{C}_s$, the inversion symmetry group $\mathcal{C}_i$; the axial groups $\mathcal{C}_n$, $\mathcal{C}_{nh}$, $\mathcal{C}_{nv}$; the dihedral groups $\mathcal{D}_n$, $\mathcal{D}_{nh}$, $\mathcal{D}_{nd}$; the cyclic groups $\mathcal{S}_{2n}$; the icosahedral groups $\mathcal{I}$, $\mathcal{I}_h$; the cubic groups $\mathcal{T}$, $\mathcal{T}_h$, $\mathcal{T}_d$, $\mathcal{O}$, $\mathcal{O}_h$. The symmetry operations are: proper rotation by $2\pi/n$ about an axis, C_n, and improper rotation, S_n (C_n followed by reflection in a plane perpendicular to the axis). By convention, the identity $E \equiv C_1$, inversion $i \equiv S_2$, and reflections $\sigma \equiv S_1$ are treated separately in character tables, each having their own column.

The scalar counting equations have straightforward extensions for systems with non-trivial point-group symmetry, constructed by replacing each scalar count with an appropriate reducible representation. Sets of structural components, internal coordinates, local translations and rotations, mechanisms and states of self stress have characters $\chi(S)$ under the various symmetry operations S of the point group $\mathcal{G}$, which define their representations Γ.

In the equations that follow below, $\Gamma(m)$ and $\Gamma(s)$ are representations of mechanisms and states of self-stress of a framework, respectively. The permutation representation of a given set of points $\{p\}$ is $\Gamma(p)$, which has entry $\chi(S)$ equal to the number of points in the set that remain unshifted when the symmetry operation S is applied to the framework. Standard named representations include: Γ_T and Γ_R for the sets of translations and rotations in the d-dimensional space; Γ_0, the totally symmetric representation, which has $\chi(S) = 1$ for all S. (See standard texts and sets of character tables, e.g., Bishop (1973); Atkins et al. (1970); Altmann and Herzig (1994).) Various derived representations can be defined for vectors or other decorations attached to components of the structure.

In these terms, a framework has a *mobility representation*, $\Gamma(m) - \Gamma(s)$, which is governed by reducible representations based on the vertices and edges of the geometrically realised contact graph. For the regular cases (d, k) we obtain three similar equations.

For $d = 3$ and $k = 3$ or 2 (Guest et al., 2010)

$$\Gamma(m) - \Gamma(s) = (\Gamma_T + \Gamma_R) \times (\Gamma(v) - \Gamma_0) - \Gamma(e); \tag{3.1}$$

for $d = 3$, $k = 1$

$$\Gamma(m) - \Gamma(s) = (\Gamma_T + \Gamma_R) \times (\Gamma(v) - \Gamma_0) - \Gamma_{\odot}(v) - \Gamma(e); \tag{3.2}$$

for $d = 3$, $k = 0$ (Fowler and Guest, 2000)

$$\Gamma(m) - \Gamma(s) = (\Gamma_T + \Gamma_R) \times (\Gamma(v) - \Gamma_0) - \Gamma(v) \times \Gamma_R - \Gamma(e). \tag{3.3}$$

In these equations, (3.2) and (3.3) are modifications of (3.1) in which further restrictions described by functions of the vertex representation are subtracted from the representation of the freedoms. In general, the count $m - s$ is replaced by the representation of freedoms of the generalised bodies, minus that

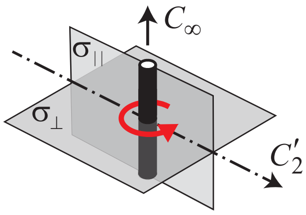

$\mathcal{D}_{\infty h}$	E	$2C_\infty(\phi)$	C_2	$\infty\sigma_\parallel$	$\sigma_\perp$	$2S_\infty(\phi)$	i	$\infty C_2'$
$\Gamma_\odot$	$+1$	$+1$	$+1$	-1	$+1$	$+1$	$+1$	-1

Figure 2: Local rotational freedom of a rod about its main axis, modelled by a circular arrow. The character for the representation $\Gamma_\odot(v)$ in the maximum site symmetry, $\mathcal{D}_{\infty h}$, is given in the table beside the figure. In practice, the site group is typically much smaller.

of the constraints imposed by the bars and that of the rigid-body motions. Equations (3.1) and (3.3) have become standard (see Guest et al. (2010) and Fowler and Guest (2000)), though (3.3) has been rewritten here to emphasise the commonality of the three equations. The equation (3.2) for symmetric rod-bar frameworks has not been presented before.

The representation $\Gamma_\odot(v)$ in Eq. (3.2) is the reducible representation of a set of circular arrows, one for each rod, about the respective rod axis, to stand for a local rotation of the rod about that axis. If $\Gamma(v)$ has $\chi(S) = 0$, then $\chi_\odot(S) = 0$; if $\chi(S) \neq 0$, then $\chi_\odot(S)$ is the sum over all unshifted rods of the entries for S in the table in Figure 2.

4. Examples of rod-bar frameworks

As examples of the formalism, we analyse some basic cases of rod-bar frameworks using our symmetry-extended counting rules.

4.1. A simple case

The first example is the rod-bar framework with $\mathcal{C}_2$ point-group symmetry that is shown in Figure 3. It has four rods, two of which are unshifted by the half-turn (one lies along the rotation axis and the other is perpendicular to, and centred on, the axis). Moreover, it has 14 bars, none of which is unshifted by the half-turn. Hence, the structure has an isostatic scalar count of $e = 5v - 6 = 14$ and a symmetry-extended count of

$$\Gamma(m) - \Gamma(s) = (6, -2) \times (3, 1) - (4, 0) - (14, 0) = (0, -2). \quad (4.1)$$

In this equation we use the pair notation (i, j) as a shorthand to indicate the character of the appropriate reducible representation under the operations in the two classes of the point group, in this case the single-element classes E and C_2 of the point group $\mathcal{C}_2$. The detailed tabular calculation for (4.1) is given below.

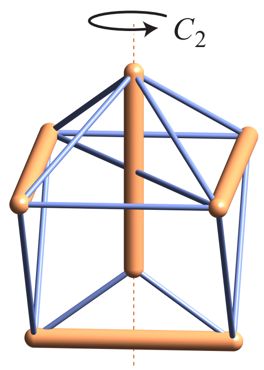

Figure 3: A rod-bar framework with an isostatic scalar count that has an infinitesimal motion and a state of self-stress, both detected by calculations of the symmetry-extended mobility count. In this and subsequent figures, rods are schematically depicted as 'wooden', and bars as 'metallic'.

$\mathcal{C}_2$	E	C_2
$\Gamma(v)$	4	2
$-\Gamma_0$	-1	-1
$\Gamma(v) - \Gamma_0$	3	1
$\times(\Gamma_T + \Gamma_R)$	6	-2
$(\Gamma(v) - \Gamma_0) \times (\Gamma_T + \Gamma_R)$	18	-2
$-\Gamma_{\odot}(v)$	-4	0
$-\Gamma(e)$	-14	0
$\Gamma(m) - \Gamma(s)$	0	-2

As $\Gamma(m) - \Gamma(s) = (0, -2) = A_2 - A_1$, we can conclude that the structure has a fully-symmetric self-stress and an anti-symmetric mechanism, neither evident from counting alone.

4.2. High-symmetry cases

The examples in this section are versions of the well known 'icosahedral tensegrity' framework, treated here as rod-bar systems. The original, analysed in Calladine (1978) and discussed in Figure 11.3 of Connelly and Guest (2022), and two variants are illustrated in Figure 4(a)–(c).

The framework in Figure 4(a) has scalar count $m - s = 5v - 6 - e = 0$, as it has $v = 6$ rods (vertices in the contact graph), and $e = 24$ bars/cables (edges of the contact graph). The framework in Figure 4(b) is a variant of (a) in which two bars/cables meet at the centre of each rod, and the framework in Figure 4(c) is a second variant in which the points of contact of bars/cables with the rods are offset in a symmetrical manner that nevertheless destroys the mirror symmetries, hence leading to a chiral configuration overall.

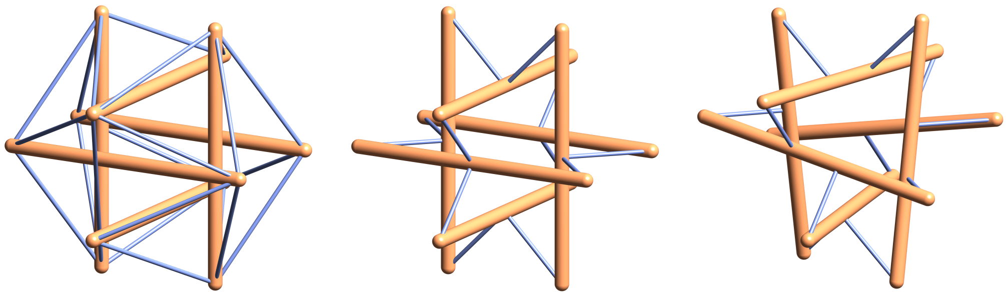

(a) (b) (c)

Figure 4: Some highly symmetrical frameworks: (a) the icosahedral tensegrity, which consists of members carrying compression and bars carrying tension, and has maximum $\mathcal{T}_h$ symmetry; (b) a variant of (a) in which compression members have been replaced by rods, and the bars now link the ends of rods to the centres of others; (c) a variant of (b) obtained by offsetting the points of attachment from rod centres, thus destroying all improper elements of symmetry and reducing the point group of the configuration from centrosymmetric $\mathcal{T}_h$ to $\mathcal{T}$. In fact, the bars in all three examples could be stressed to carry only tension and hence could be replaced by cables in all cases.

For (a) and (b), the overall point group is $\mathcal{T}_h$. For (c), the overall point group is $\mathcal{T}$. Structures (b) and (c) share the scalar count $m-s = 5v-6-e = 12$, as both have $v = 6$ and $e = 12$.

The arrangements of rods with respect to symmetry elements in the $\mathcal{T}_h$-symmetric (a) and (b) are identical, and so the calculation of the freedom term, i.e. $(\Gamma_T + \Gamma_R) \times (\Gamma(v) - \Gamma_0) - \Gamma_\odot(v)$, is the same for both systems. As the first part of the table for (b) (below) shows, the result is the regular representation $\Gamma_{\text{reg}}(\mathcal{T}_h)$, which has character $|\mathcal{T}_h| = 24$ under the identity but character zero elsewhere, reducing to $A_g + E_g + 3T_g + A_u + E_u + 3T_u$ in this separably degenerate point group.

The difference between the two $\mathcal{T}_h$ systems lies in the constraint term. Framework (a) has 24 edges of the contact graph, none of which lies on an element of symmetry, and $\Gamma(e)$ is therefore equal to $\Gamma_{\text{reg}}(\mathcal{T}_h)$. Hence, for framework (a), the mobility representation is null, implying that in the $\mathcal{T}_h$

configuration the system has equal numbers of mechanisms and states of self stress and that the two sets are equisymmetric. In fact, the framework (a) has $\Gamma(m) = \Gamma(s) = A_g$ (Guest, 2011).

Framework (b) is more interesting as a 12−dimensional constraint representation clearly cannot cancel the 24−dimensional representation of the freedoms. As the full calculation for (b) shows, the mobility representation $\Gamma(m) - \Gamma(s)$ is $2T_g + A_u + E_u + T_u$, accounting for the excess of 12 independent infinitesimal motions predicted from the scalar count:

$\mathcal{T}_h$	E	$4C_3$	$4C_3^2$	$3C_2$	i	$4S_6$	$4S_6^2$	$3\sigma_d$
$\Gamma(v)$	6	0	0	2	0	0	0	4
$-\Gamma_0$	−1	−1	−1	−1	−1	−1	−1	−1
$\Gamma(v) - \Gamma_0$	5	−1	−1	1	−1	−1	−1	3
$\times(\Gamma_T + \Gamma_R)$	6	0	0	−2	0	0	0	0
$(\Gamma(v) - \Gamma_0) \times (\Gamma_T + \Gamma_R)$	30	0	0	−2	0	0	0	0
$-\Gamma_\odot(v)$	−6	0	0	2	0	0	0	0
$-\Gamma(e)$	−12	0	0	0	0	0	0	−4
$\Gamma(m) - \Gamma(s)$	12	0	0	0	0	0	0	−4

Framework (c) has only $\mathcal{T}$ symmetry, and the tabular character calculation is simply halved, as $\mathcal{T}_h$ reduces to $\mathcal{T}$ on deletion of improper symmetry operations. As the centres of the rods are in the same positions as in (a) and (b) (the vertices of an inscribed octahedron), the freedoms span two copies of the regular representation in the smaller point group, but now the 12 constraints span $\Gamma_{\mathrm{reg}}(\mathcal{T})$, and the mobility representation for framework (c) is $A + E + 3T$, as would be obtained by a descent-in-symmetry argument from the result for (b).

Again, we do not detect any additional infinitesimal motions with the symmetry-extended counting rule, but do obtain useful information about the nature of the 12 independent motions predicted by the scalar count. In no case (a) to (c) does the symmetry analysis detect states of self stress, although it is evident that these exist, from both physical models and equilibrium calculations.

5. When is a symmetric rod-bar framework isostatic?

Isostatic structures play important roles in engineering since they are able to react to changes in shape of their structural components by deforming without building up states of self-stress. In an isostatic framework, there are neither mechanisms nor states of self-stress, and so $m - s = 0$; in the symmetry approach, this implies the character equality $\Gamma(m) - \Gamma(s) = 0$. Using an established approach (Connelly et al., 2009; Guest et al., 2010), we derive necessary conditions for a symmetric rod-bar framework to be isostatic. These isostaticity conditions are given in the form of simply stated restrictions on the numbers of those structural components that are unshifted by the symmetry operations of the framework.

Calculation of characters for the 3D symmetry-extended 'rod-bar' equation (recall Eq. (3.2)) is shown in Table 1. Characters are calculated for six types of operation: for proper rotations, we distinguish E and C_2 from the C_n operations with $n > 2$; for improper rotations, we distinguish σ and i from the S_n operations with $n > 2$. The notation used describes the local symmetries of the vertices and edges of the contact graph as follows:

	E	σ	i	$S_{n>2}$	C_2	$C_{n>2}(\phi)$
$\Gamma(v)$	v	v_σ	v_c	v_{nc}	v_2	v_n
$-\ \Gamma_0$	-1	-1	-1	-1	-1	-1
$= \Gamma(v) - \Gamma_0$	$v-1$	$v_\sigma - 1$	$v_c - 1$	$v_{nc} - 1$	$v_2 - 1$	$v_n - 1$
$\times\ (\Gamma_T + \Gamma_R)$	6	0	0	0	-2	$4\cos\phi + 2$
$= (\Gamma(v) - \Gamma_0) \times (\Gamma_T + \Gamma_R)$	$6(v-1)$	0	0	0	$-2(v_2 - 1)$	$(4\cos\phi + 2)(v_n - 1)$
$-\ \Gamma(e)$	$-e$	$-e_\sigma$	$-e_c$	$-e_{nc}$	$-e_2$	$-e_n$
$-\ \Gamma_\odot(v)$	$-v$	$v_{\sigma\parallel} - v_{\sigma\perp}$	$-v_c$	$-v_{nc}$	$v_{2\perp} - v_{2\parallel}$	$-v_n$

Table 1: Calculation of the mobility representation $\Gamma(m) - \Gamma(s)$ for the symmetry-extended rod-bar equation (3.2) for rod-bar frameworks in 3-space. The vertices and edges here are those of the contact graph, $\mathcal{C}$, in which a vertex of $\mathcal{C}$ corresponds to a rod, and an edge of $\mathcal{C}$ to a bar. $C_n(\phi)$ is a rotation through $\phi = 2\pi/n$. Subscript notation is explained in the text. The sum of the three final rows corresponds to the mobility representation $\Gamma(m) - \Gamma(s)$.

v is the total number of rods;

v_n is the number of rods that are unshifted by a given n-fold rotational symmetry operation $C_{n\geq 2}$. For $n = 2$, each such rod either lies along the C_2 axis or perpendicular to, and centred on, the C_2 axis. For $n > 2$, each such rod lies along the C_n axis;

$v_{2\|}$ is the number of rods that lie along the C_2 axis;.

$v_{2\perp}$ is the number of rods that lie perpendicular to, and centred on, the axis;

v_c is the number of rods unshifted by the inversion i; each such rod is centred on the unique central point, but no particular orientation is implied;

v_{nc} is the number of rods unshifted by the improper rotation $S_{n>2}$; each such rod must lie along the axis of the rotation, and be centred in the central point of the group;

v_σ is the number of rods unshifted by a given reflection σ. Each such rod either lies within the σ plane or perpendicular to, and centred in, the σ plane;

$v_{\sigma\|}$ is the number of rods that lie within the σ plane;

$v_{\sigma\perp}$ is the number of rods that lie perpendicular to, and centred in, the σ plane;

e is the total number of bars;

e_n is the number of bars unshifted by a $C_{n\geq 2}$ rotation. For $n = 2$, each such bar must lie either along, or perpendicular to and centred on the axis.

For $n > 2$, each such bar must lie along the C_n-axis;

e_c is the number of bars unshifted by the inversion i; the centre of the bar must lie at the central point of the group, but no particular orientation is implied;

e_{nc} is the number of bars unshifted by the improper rotation $S_{n>2}$; such bars must lie along the axis of the rotation, and be centred on the central point of the group;

e_σ is the number of bars unshifted by a given reflection σ; an unshifted bar may lie within the mirror or perpendicular to and centred on the mirror.

Each count refers to a particular symmetry element, and so, for instance a rod counted in v_c also contributes to v, and may contribute to v_n and v_σ if these symmetries are present.

From Table 1, the symmetry treatment of the 3D rod-bar equation reduces to six scalar equations. If $\Gamma(m) - \Gamma(s) = 0$, then

E: $$5v - 6 = e \tag{5.1}$$

σ: $$v_{\sigma\parallel} - v_{\sigma\perp} = e_\sigma \tag{5.2}$$

i: $$-v_c = e_c \tag{5.3}$$

$S_{n>2}$: $$-v_{nc} = e_{nc} \tag{5.4}$$

C_2: $$2 - 2v_2 - v_{2\parallel} + v_{2\perp} = e_2 \tag{5.5}$$

$C_{n>2}$: $$(v_n - 1)(4\cos\phi + 2) - v_n = e_n \tag{5.6}$$

where a given equation applies when the corresponding symmetry operation is present in $\mathcal{G}$.

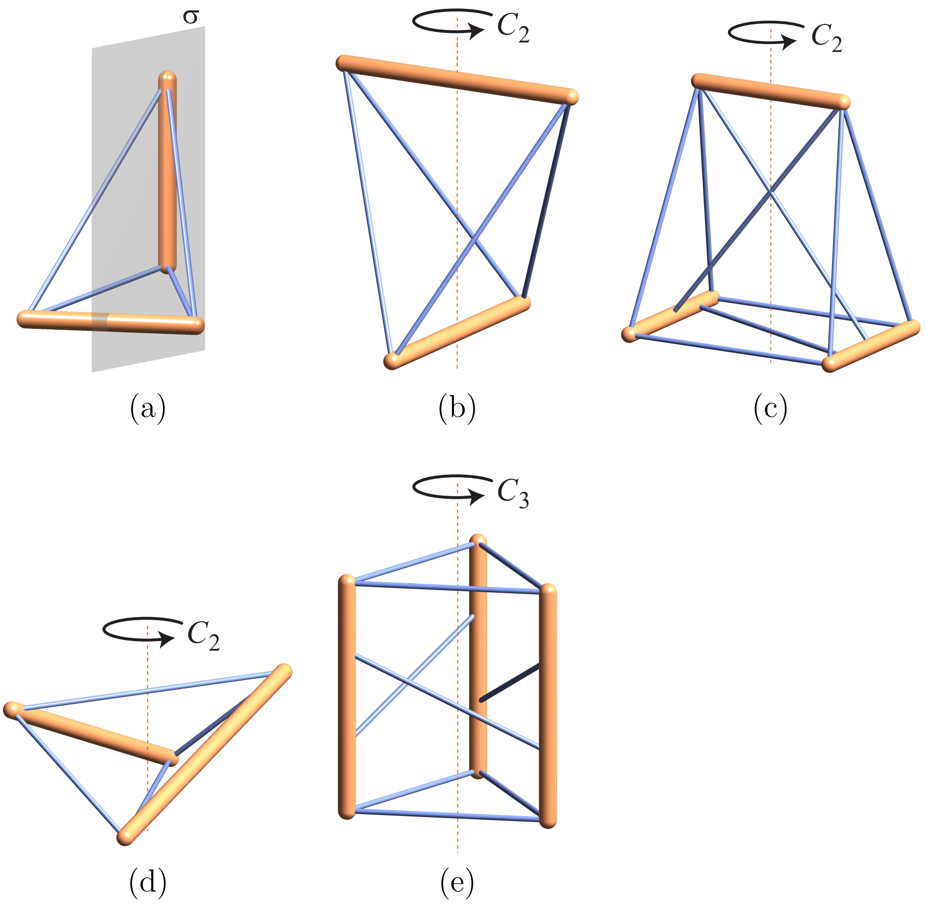

Figure 5: Isostatic symmetric rod-bar frameworks, with their point-group symmetries ((a) $\mathcal{C}_s$; (b),(c),(d) $\mathcal{C}_2$; (e) $\mathcal{C}_3$), exemplifying the various structural counting rules derived in the text.

Some observations on 3D isostatic rod-bar frameworks, arising from the above, are as follows:

(i) From (5.1), the rod-bar framework must satisfy the scalar rule with $m - s = 0$: $5v - 6 = e$ (recall §2);

(ii) From (5.2), for each mirror σ that is present we must have $v_{\sigma\|} \geq v_{\sigma\perp}$; In particular, if $v_{\sigma\|} = 0$ then we also have $v_{\sigma\perp} = 0$ and $e_\sigma = 0$. Moreover, if $v_{\sigma\perp} = 0$, then $v_{\sigma\|} = e_\sigma$;

(iii) From (5.3), a centrosymmetric rod-bar framework has no bar centred at the inversion centre, and there is also no centrally symmetric rod;

(iv) From (5.4), the presence of an improper rotation $S_{n>2}$ implies that there is no bar and no rod that is unshifted by $S_{n>2}$;

(v) For a C_2 axis, (5.5) may be written as

$$2 - 2(v_{2\|} + v_{2\perp}) - v_{2\|} + v_{2\perp} = e_2$$

since $v_2 = v_{2\|} + v_{2\perp}$. We may simplify this to

$$2 - 3v_{2\|} - v_{2\perp} = e_2$$

which implies that $v_{2\|} = 0$, as e_2 must be a non-negative integer. Therefore, $2 - v_{2\perp} = e_2$. Thus, the possible solutions are

$$(e_2, v_{2\perp}, v_{2\|}) = (0, 2, 0), (1, 1, 0), \text{ or } (2, 0, 0).$$

(vi) Equation (5.6) can be written, with $\phi = 2\pi/n$, as

$$(v_n - 1)\left(4\cos\left(\frac{2\pi}{n}\right) + 2\right) - v_n = e_n$$

with $n > 2$. It follows immediately that v_n must be distinct from 1. Note that the factor $(4\cos(2\pi/n) + 2)$ is rational only for $n = 3, 4, 6$. We consider each case in turn:

$n = 3$

$$-v_3 = e_3$$

and so here $v_3 = e_3 = 0$. A C_3 axis may be present, but if so, no vertices or edges of $\mathcal{C}$ lie on it.

$n = 4$

$$v_4 - 2 = e_4$$

It follows that $v_4 \geq 2$. However, this is impossible since $v_4 \geq 2$ implies that $v_{2\parallel} \geq 2$. Thus, a 4-fold rotation C_4 is not present.

$n = 6$

$$3v_6 - 4 = e_6$$

It follows that $v_6 \geq 1$. However, this is impossible since $v_6 \geq 1$ implies that $v_{2\parallel} \geq 1$. Thus, a 6-fold rotation C_6 is not present.

In summary of this case, we can see that only a C_3 rotational axis is compatible with isostaticity, albeit with further restrictions.

Examples of symmetric rod-bar frameworks with isostatic scalar counts are shown in Figure 5.

6. Symmetry-extended mobility count for rod-clamp frameworks

A natural specialisation of rod-bar frameworks is their restriction to *rod-clamp* frameworks. This is similar in spirit to what is typically done in going from body-bar to *body-hinge* frameworks. To model a clamp we consider a pair of rods that are connected by three orthogonal bars that all meet in a common point and have zero length in the limiting case when the rods touch. Rod-clamp structures were studied as mathematical objects by Tay (Tay, 1991, 1989) and they give a natural formalisation of the physical structures made in scouting, woodcraft and nautical contexts by lashing rods together to make tripods, towers and other improvised structures. Rod-clamp structures have recently also been used in the rigidity analysis of composite materials and fiber networks (Heroy et al., 2022). 'Popsicle bombs' give another motivation for the study of rod-clamp frameworks; the underlying grillage in this popular impromptu toy is the polar of a tensegrity (Whiteley, 1989; Schulze and Whiteley, 2023) in which a state of self-stress blocks the eponymous disruptive mechanism (Tarnai, 1989).

The essential feature of a *clamp* is that rods in their disconnected state have five degrees of freedom each, and each incidence of two rods connected via a clamp removes three degrees of freedom for the pair (relative translations of the two rods). The Maxwell count of a 3D rod-clamp framework is therefore

$$m - s = 5v - 6 - 3c \tag{6.1}$$

where c is the number of clamps and v, m, s are the respective numbers of rods, mechanisms and states of self-stress, as before.

As usual, this scalar relation has a symmetry-extended counterpart that follows from the construction of the general rod-bar equation (3.2) for regular frameworks as

$$\Gamma(m) - \Gamma(s) = (\Gamma_T + \Gamma_R) \times (\Gamma(v) - \Gamma_0) - \Gamma_\odot(v) - \Gamma(c), \tag{6.2}$$

where $\Gamma(c)$ stands for the (reducible) representation of the freedoms removed by the set of clamps.

Calculation of $\Gamma(c)$ for a set of clamps distributed in space takes a well trodden path. The representation spanned by the relative translations of a pair of rods is calculated for configurations of high symmetry, interpreted in terms of decorations of clamp positions with a set of local motifs, and then used to calculate the contribution to $\Gamma(c)$ of each clamp unshifted by a given symmetry operation. For clamps that are shifted out of position by the operation, the contribution is zero.

A pair of rods, in the idealisation of zero thickness, has maximum D_{4h} site symmetry for intersection at 90°, and D_{2h} symmetry for non-orthogonal intersection, dropping to C_{2v} and C_s when one or more rods are not centred on the clamp. Figure 6 gives a pictorial description of the local symmetries of the three excluded relative translations, and Table 2 shows their representations in the respective maximal groups. The arguments used to derive the entries in these mini character tables follow closely those used for symmetry descriptions of CAD constraints in point-line systems, as described in Fowler et al. (2021).

As examples of the approach, we consider first the 3D frameworks illustrated schematically and shown as physical models in Figure 7. Rows (a) and (b) in Figure 7 show two rod-clamp frameworks that have the isostatic count $m - s = 0$, as they both have $v = 6$ rods and $c = 8$ clamps. The structure in (a) has reflection symmetry and the symmetry-adapted count (6.2) detects a fully-symmetric infinitesimal motion, which is in fact finite, as illustrated by the different configurations of the model shown in (c) and (d). The structure in (b) has half-turn symmetry and the symmetry-adapted count is isostatic; the physical model is rigid.

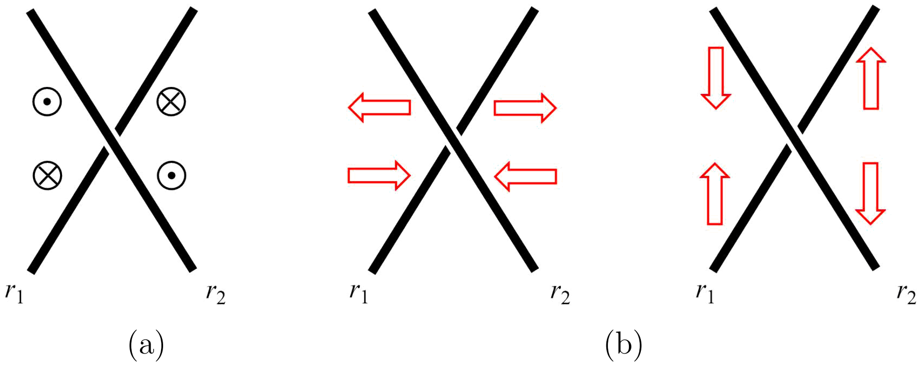

Figure 6: The three degrees of freedom (relative translations) that are removed by a clamp connecting two rods r_1 and r_2: (a) the out-of-plane ($\perp$) translation that separates the two rods; (b) a pair of in-plane ($\|$) translations corresponding to slides of one rod against the other. Decorations of the clamp with sets of four arrows show the local symmetry of the freedom. We consider the two bars to be coincident at the clamping point, and ignore the question of which rod is above, and which below in a given physical realization.

For the structure in (a) with $\mathcal{C}_s$ symmetry we obtain the count

$$\Gamma(m) - \Gamma(s) = (6,0) \times [(6,0) - (1,1)] - (6,0) - (24,-2) = (0,2):$$

$\mathcal{C}_s$	E	σ
$\Gamma(v)$	6	0
$-\Gamma_0$	-1	-1
$\Gamma(v) - \Gamma_0$	5	-1
$\times(\Gamma_T + \Gamma_R)$	6	0
$(\Gamma(v) - \Gamma_0) \times (\Gamma_T + \Gamma_R)$	30	0
$-\Gamma_{\odot}(v)$	-6	0
$-\Gamma(c)$	-24	2
$\Gamma(m) - \Gamma(s)$	0	2

As $\Gamma(m) - \Gamma(s) = (0,2) = A' - A''$, we can conclude that the structure

(i)

$\mathcal{D}_{4h}$	E	$2C_4$	C_2	$2C_2'$	$2C_2''$	i	$2S_4$	σ_h	$2\sigma_v$	$2\sigma_d$
$\Gamma(c_\perp)$	$+1$	-1	$+1$	$+1$	-1	-1	$+1$	-1	-1	$+1$
$\Gamma(c_\parallel)$	$+2$	0	-2	0	0	-2	0	$+2$	0	0

(ii)

$\mathcal{D}_{2h}$	E	C_{2z}	C_{2x}	C_{2y}	i	σ_z	σ_x	σ_y
$\Gamma(c_\perp)$	$+1$	$+1$	$+1$	$+1$	-1	-1	-1	-1
$\Gamma(c_\parallel)$	$+2$	-2	0	0	-2	$+2$	0	0

Table 2: Calculation of representation $\Gamma(c)$ as a constraint that removes all local relative translations of two clamped rods. The characters are calculated in the highest possible symmetry group: (i) $\mathcal{D}_{4h}$ for centred mutually perpendicular rods, and (ii) $\mathcal{D}_{2h}$ for centred rods meeting at an arbitrary angle. Following the illustration in Fig. 6, $\Gamma(c)$ decomposes into a constraint that fixes the separation at zero, with representation $\Gamma(c_\perp)$, and a reducible representation $\Gamma(c_\parallel)$ that describes the pair of constraints on relative translations in the orthogonal plane. The calculation for the subgroups $\mathcal{C}_{2v}$ and $\mathcal{C}_s$ is carried out using the same tables, but with columns restricted to the symmetry elements present in the subgroup.

has a fully-symmetric infinitesimal motion and an anti-symmetric self-stress.

For the structure (b), which has $\mathcal{C}_2$ symmetry, we obtain the count

$$\Gamma(m) - \Gamma(s) = (6, -2) \times [(6, 2) - (1, 1)] - (6, -2) - (24, 0) = (0, 0)$$

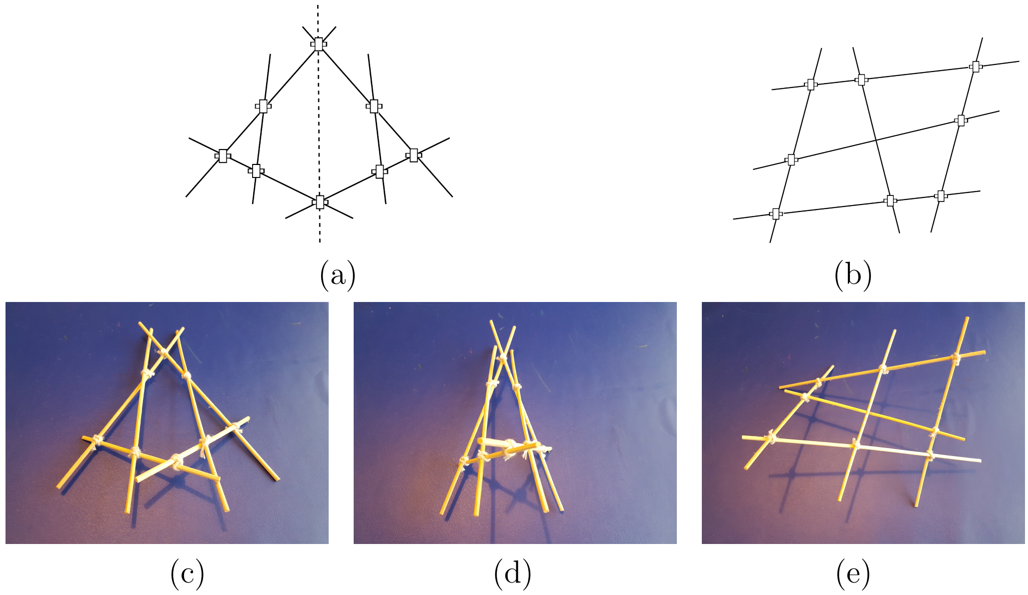

Figure 7: (a),(b) Top-down view of 3D rod-clamp frameworks of $\mathcal{C}_s$ and $\mathcal{C}_2$ symmetry with $m - s = 0$. Sets of vertices under the appropriate two-fold symmetry each have a fixed but arbitrary height in the missing third dimension. Clamps are indicated by the symbol . (c),(d) Different configurations of a physical model of the structure shown in (a). (e) Physical model of the structure shown in (b). There is no clamp at the central crossing, where the bars are separated in the out-of-page dimension.

$\mathcal{C}_2$	E	C_2
$\Gamma(v)$	6	2
$-\Gamma_0$	-1	-1
$\Gamma(v) - \Gamma_0$	5	1
$\times(\Gamma_T + \Gamma_R)$	6	-2
$(\Gamma(v) - \Gamma_0) \times (\Gamma_T + \Gamma_R)$	30	-2
$-\Gamma_{\odot}(v)$	-6	2
$-\Gamma(c)$	-24	0
$\Gamma(m) - \Gamma(s)$	0	0

From both scalar and symmetry-extended counts, this structure appears rigid. In the flattened structure, which would have $\mathcal{C}_{2h}$ symmetry, the mobility representation $\Gamma(m) - \Gamma(s)$ would be $(0, 0, -2, -2)$, indicating an infinitesimal out-of-plane mechanism of A_u symmetry that would be blocked in non-planar configurations by the totally symmetric A_g state of self-stress.

We note that the structure in Figure 7(a) will remain flexible even if it is perturbed so that the reflection symmetry is broken, because the line through the top and bottom clamp acts as a hinge line. This is analogous to the well known surprising motion of the "double-banana" framework, for which a symmetry treatment is given in Fowler and Guest (2002).

7. Mixed body-panel-rod frameworks

Non-regular plate-bar frameworks in 3-space that contain a mix of rods and 2- or 3-dimensional bodies are common in engineering. For these mixed 'body-panel-rod' frameworks, the Maxwell count in Equation (2.2) from Section 2 simplifies to

$$m - s = 6v - v_{\text{rod}} - 6 - e,$$

where v and e are the numbers of vertices and edges of the contact graph and v_{rod} is the number of vertices in the contact graph corresponding to rods. A symmetry-adapted mobility count for these structures is easily obtained by modifying Equation (3.2) from Section 3 as follows:

$$\Gamma(m) - \Gamma(s) = (\Gamma_T + \Gamma_R) \times (\Gamma(v) - \Gamma_0) - \Gamma_{\odot}(v_{\text{rod}}) - \Gamma(e). \tag{7.1}$$

To illustrate this counting rule, we apply it to two symmetric configurations of the linear pentapod, which is a structure consisting of a rod (a linear-motion platform) that is connected to a base by 5 bars (see e.g. Borràs et al. (2011); Rasoulzadeh and Nawratil (2019)). Figure 8 shows two symmetric configurations of this structure. Linear pentapods have a wide range of industrial applications (Borràs and Thomas, 2010; Weck and Staimer, 2002) and can be thought of as modified Stewart-Gough platforms, where the platform has been replaced by a rod and one of the six connecting bars has been removed to maintain an isostatic Maxwell count.

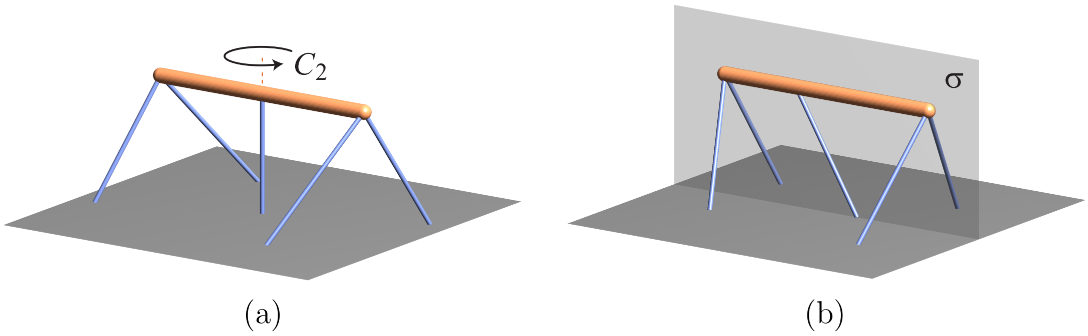

Figure 8: Two symmetric configurations of the linear pentapod, one with half-turn symmetry (a) and one with reflection symmetry (b).

For the structure in Figure 8(a) with half-turn symmetry we obtain the count

$$\Gamma(m) - \Gamma(s) = (6, -2) \times [(2, 2) - (1, 1)] - (1, -1) - (5, 1) = (0, -2)$$

as detailed in the tabular calculation below.

$\mathcal{C}_2$	E	C_2
$\Gamma(v)$	2	2
$-\Gamma_0$	-1	-1
$\Gamma(v) - \Gamma_0$	1	1
$\times(\Gamma_T + \Gamma_R)$	6	-2
$(\Gamma(v) - \Gamma_0) \times (\Gamma_T + \Gamma_R)$	6	-2
$-\Gamma_{\odot}(v_{\mathrm{rod}})$	-1	1
$-\Gamma(e)$	-5	-1
$\Gamma(m) - \Gamma(s)$	0	-2

Since $\Gamma(m) - \Gamma(s) = (0, -2) = -A_1 + A_2$, we can conclude that the structure has a fully-symmetric self-stress and an anti-symmetric infinitesimal motion in which the centre of the rod moves in a direction perpendicular to the central bar,

For the structure in Figure 8(b) with reflection symmetry, we have

$$\Gamma(m) - \Gamma(s) = (6, 0) \times [(2, 2) - (1, 1)] - (1, -1) - (5, 1) = (0, 0)$$

as detailed in the tabular calculation below.

$\mathcal{C}_s$	E	σ
$\Gamma(v)$	2	2
$-\Gamma_0$	-1	-1
$\Gamma(v) - \Gamma_0$	1	1
$\times(\Gamma_T + \Gamma_R)$	6	0
$(\Gamma(v) - \Gamma_0) \times (\Gamma_T + \Gamma_R)$	6	0
$-\Gamma_{\odot}(v_{\mathrm{rod}})$	-1	1
$-\Gamma(e)$	-5	-1
$\Gamma(m) - \Gamma(s)$	0	0

Thus, the symmetry-adapted count does not detect self-stresses or motions, and the structure is in fact isostatic whenever it is placed generically with respect to the constraints given by the reflection symmetry. The difference in mobility count for the two cases derives entirely from the different behaviour of the representation of the rigid-body motions $\Gamma_T + \Gamma_R$: the trace of this reducible representation can be non-vanishing under a proper symmetry operation, but is necessarily zero under an improper symmetry operation.

8. Sufficient conditions for symmetry-generic isostaticity

The Maxwell count $|E| = [\binom{d+1}{2} - 1]|V| - \binom{d+1}{2}$ is clearly necessary for the $(d, d-2)$-plate-bar framework with contact graph $\mathcal{C} = (V, E)$ to be isostatic. (Recall (2.2) and the discussion in Section 2; here we are using V, E as shorthand for $V(\mathcal{C})$ and $E(\mathcal{C})$ from that discussion.) It was shown by Tay that this count, together with the corresponding sparsity counts for all non-trivial subgraphs of $\mathcal{C}$, is also *sufficient* for generic realisations of $\mathcal{C}$ as a

$(d, d-2)$-plate-bar framework to be isostatic (Tay, 1989, 1991).

Theorem 8.1 (Tay, 1989)**.** *Let $d \geq 2$. Then a generic $(d, d-2)$-plate-bar framework is isostatic if and only if the contact graph $\mathcal{C} = (V, E)$ is $\left(\binom{d+1}{2} - 1, \binom{d+1}{2}\right)$-tight, i.e.*

$$|E| = \left[\binom{d+1}{2} - 1\right]|V| - \binom{d+1}{2}$$

and

$$|E'| \leq \left[\binom{d+1}{2} - 1\right]|V'| - \binom{d+1}{2}$$

for all non-trivial subgraphs (V', E') of $\mathcal{C}$.

In particular, it follows from Tay's result that a generic rod-bar framework in 3-space is isostatic if and only if the contact graph is $(5, 6)$-tight. An extended theorem for mixed plate-bar frameworks with both bodies and rods in 3-space was established by Tanigawa in Tanigawa (2012). A corresponding result for generic $(d, d-3)$-plate-bar frameworks for $d \geq 3$ has not yet been established.

Given a rod-bar framework with a non-trivial point group symmetry, it is clear that $(5, 6)$-tightness of the contact graph is still a necessary condition for the framework to be isostatic. We have seen in Section 5 that there are additional necessary conditions which are given in terms of the number of structural components that are unshifted by the symmetry operations of the structure. It is natural to ask whether for a point group $\mathcal{S}$ all of these conditions combined, together with the corresponding symmetry conditions for all subgraphs of the contact graph with symmetry $\mathcal{S}' \subseteq \mathcal{S}$, are sufficient for a realisation of the contact graph as a rod-bar framework to be isostatic as long as it is as generic as possible with the given symmetry constraints. It turns out that in general this is not the case.

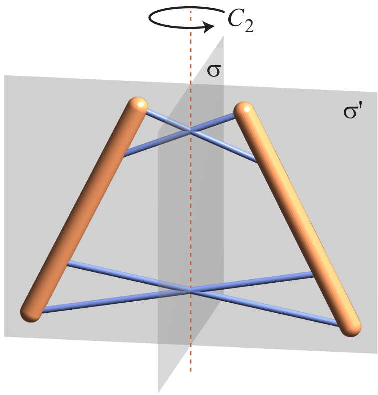

Figure 9: A rod-bar framework with $\mathcal{C}_{2v}$ symmetry. As it lies within the mirror plane corresponding to σ', it is not isostatic.

Consider, for example, a reflection-symmetric rod-bar framework consisting of a pair of rods that are images of each other under a reflection σ and four bars between them none of which are unshifted by σ (see Figure 9). This structure satisfies all the necessary conditions for isostaticity mentioned above. However, the reflection σ forces the structure to lie within a plane in 3-space and therefore to also have the reflection σ' and the half-turn rotation symmetry C_2, and hence to have the larger point-group symmetry $\mathcal{C}_{2v}$. The structure does not satisfy the isostaticity conditions for σ' and hence has a non-trivial self-stress (and also an infinitesimal motion) which are not detectable with the symmetry counts for σ alone.

Finally, we note that while necessary counts for isostaticity of rod-clamp frameworks have been obtained, a full combinatorial theory (even without symmetry) has not yet been developed for these structures. See (Nixon et al., 2021, Section 9.6), for example, for a discussion.

9. Conclusions

The work described here is part of a research programme based on the realisation that consideration of non-trivial symmetries of a framework can give useful information about the balance of freedoms and constraints, and qualitative 'selection rules' for mechanisms and states of self-stress. Classical counting rules state necessary conditions for rigidity, and in favourable cases, non-trivial point-group symmetry implies further counting rules, each related to a class of symmetry elements.

In particular, the current paper has generalised the symmetry treatment for the wide class of systems that is covered by the umbrella term of plate-bar frameworks, which are of interest in applications from tensegrities to robotics. The symmetry-extended Maxwell equation for the plate-bar framework has been derived, together with an easily applied template for determination of representations of constraints in plate-bar systems, and codification of the class-by-class counting rules. This allowed a full classification of the implication of different symmetry elements (mirrors, half-turns and higher rotations) for isostatic behaviour in 3D rod-bar systems. Even for the low point groups typical of robotic platforms, it was shown that symmetry conslderations can often detect mechanisms. A full specification of sufficient conditions for symmetry-generic isostaticity of plate-bar systems is, however, still to be achieved.

Use of a symmetry-adapted method pre-supposes detection of point-group symmetry in a presented structure. This is often straightforward. Recognition of symmetries of structures is a useful skill acquired by students in disciplines such as chemistry, physics and materials science. Automated detection of symmetry is implemented in most large software packages for electronic structure and crystallographic analysis, for example, and has been proposed for engineering-type structures (Zingoni, 2012). All the examples quoted in the present paper were simple enough for the symmetry analysis to be performed and implemented by hand.

References

Altmann, S. L. and Herzig, P. (1994). *Point-Group Theory Tables*. Clarendon Press, Oxford.

Asimow, L. and Roth, B. (1979). The rigidity of graphs. II. *J. Math. Anal. Appl.*, 68(1):171–190.

Atkins, P. W., Child, M. S., and Phillips, C. S. G. (1970). *Tables for Group Theory*. Oxford University Press.

Bishop, D. M. (1973). *Group Theory and Chemistry*. Clarendon Press, Oxford.

Borràs, J. and Thomas, F. (2010). Singularity-invariant leg substitutions in pentapods. In *2010 IEEE/RSJ International Conference on Intelligent Robots and Systems*, pages 2766–2771.

Borràs, J., Thomas, F., and Torras, C. (2011). Architectural singularities of a class of pentapods. *Mechanism and Machine Theory*, 46(8):1107–1120.

Calladine, C. R. (1978). Buckminster Fuller's "Tensegrity" structures and Clerk Maxwell's rules for the construction of stiff frames. *International Journal of Solids and Structures*, 14:161–172.

Chen, Y., Feng, J., and Liu, Y. (2016). A group-theoretic approach to the mobility and kinematic of symmetric over-constrained structures. *Mechanism and Machine Theory*, 105:91–107.

Chen, Y., Guest, S., Fowler, P., and Feng, J. (2012). Two-orbit switch-pitch structures. *Journal of the International Association for Shell and Spatial Structures*, 53:157–162.

Connelly, R., Fowler, P. W., Guest, S. D., Schulze, B., and Whiteley, W. J. (2009). When is a symmetric pin-jointed framework isostatic? *International Journal of Solids and Structures*, 46:762–773.

Connelly, R. and Guest, S. D. (2022). *Frameworks, tensegrities, and symmetry.* Cambridge University Press, Cambridge.

Fowler, P. W. and Guest, S. D. (2000). A symmetry extension of Maxwell's rule for rigidity of frames. *International Journal of Solids and Structures*, 37:1793–1804.

Fowler, P. W. and Guest, S. D. (2002). Symmetry analysis of the double banana and related indeterminate structure. In Drew, H. R. and Pellegrino, S., editors, *New Approaches to Structural Mechanics, Shells and Biological Structures*, pages 91–100. Kluwer Academic Press, Dordrecht.

Fowler, P. W., Guest, S. D., and Owen, J. C. (2021). Applications of symmetry in point–line–plane frameworks for CAD. *Journal of Computational Design and Engineering*, 8:615–637.

Guest, S. D. (2011). The stiffness of tensegrity structures. *IMA J. Appl. Math.*, 76(1):57–66.

Guest, S. D. and Fowler, P. W. (2005). A symmetry-extended mobility rule. *Mechanism and Machine Theory*, 40:1002–1014.

Guest, S. D. and Fowler, P. W. (2007). Symmetry conditions and finite mechanisms. *Journal of Mechanics of Materials and Structures*, 2:293–301.

Guest, S. D. and Fowler, P. W. (2010). Mobility of 'N-loops'; bodies cyclically connected by intersecting revolute hinges. *Proceedings of the Royal Society A: Mathematical, Physical and Engineering Science*, 466:63–77.

Guest, S. D., Schulze, B., and Whiteley, W. J. (2010). When is a body-bar structure isostatic? *International Journal of Solids and Structures*, 47:2745–2754.

Heroy, S., Taylor, D., Shi, F., Forest, M. G., and Mucha, P. J. (2022). Rigidity percolation in disordered 3D rod systems. *Multiscale Model. Simul.*, 20(1):250–281.

Katoh, N. and Tanigawa, S. (2011). A proof of the molecular conjecture. *Discrete Comput. Geom.*, 45(4):647–700.

Kiraly, C. and Tanigawa, S. (2019). Rigidity of body-bar-hinge frameworks. In Sitharam, M., St. John, A., and Sidman, J., editors, *Handbook of geometric constraint systems principles*, Discrete Mathematics and its Applications, chapter 20. CRC, Boca Raton, FL.

Kutzbach, K. (1929). Mechanische Leitungsverzweigung. *Maschinenbau, Der Betrieb*, 8:710–716.

Maxwell, J. C. (1864). On the calculation of the equilibrium and stiffness of frames. *Philosophical Magazine.*, 27:294–299.

Nixon, A., Schulze, B., and Whiteley, W. (2021). Rigidity through a projective lens. *Applied Sciences*, pages 1–105.

Rasoulzadeh, A. and Nawratil, G. (2019). Linear pentapods with a simple singularity variety – part I: Determination and redundant designs. In Uhl, T., editor, *Advances in Mechanism and Machine Science*, pages 689–698, Cham. Springer International Publishing.

Schulze, B., Guest, S. D., and Fowler, P. W. (2014). When is a symmetric body-hinge structure isostatic? *International Journal of Solids and Structures*, 51:2157–2166.

Schulze, B. and Whiteley, W. (2023). Projective geometry of scene analysis, parallel drawing and reciprocal diagrams. in preparation.

Tanigawa, S. (2012). Generic rigidity matroids with Dilworth truncations. *SIAM J. Discrete Math.*, 26(3):1412–1439.

Tarnai, T. (1989). Duality between plane trusses and grillages. *Internat. J. Solids Structures*, 25(12):1395–1409.

Tay, T. and Whiteley, W. J. (1984). Recent advances in the generic rigidity of structures. *Structural Topology*, 9. Dual French-English text.

Tay, T. S. (1984). Rigidity of multi-graphs, linking rigid bodies in n-space. *J. Comb. Theory, B*, 36:95–112.

Tay, T. S. (1989). Linking $(n-2)$-dimensional panels in n-space II: $(n-2,2)$-frameworks and body and hinge structures. *Graphs Combin.*, 5(1):245–273.

Tay, T. S. (1991). Linking $(n-2)$-dimensional panels in n-space I: $(k-1,k)$-graphs and $(k-1,k)$-frames. *Graphs Combin.*, 7(3):289–304.

Weck, M. and Staimer, D. (2002). Parallel kinematic machine tools - current state and future potentials. *CIRP Annals - Manufacturing Technology*, 51:671–683.

Whiteley, W. (1989). Rigidity and polarity. II. Weaving lines and tensegrity frameworks. *Geom. Dedicata*, 30(3):255–279.

Whiteley, W. J. (1996). Some matroids from discrete applied geometry. In *Matroid theory (Seattle, WA, 1995)*, volume 197 of *Contemp. Math.*, pages 171–311. Amer. Math. Soc., Providence, RI.

Whiteley, W. J. (2005). Counting out to the flexibility of molecules. *J. Physical Biology*, 2:1–11.

Zingoni, A. (2012). Symmetry recognition in group-theoretic computational schemes for complex structural systems. *Computers & Structures*, 94-95:34–44.